journal

J. Am. Ceram. Soc., **82** [5] 1318–24 (1999)

Effect of Preparation Conditions on Phase Formation, Densification, and Microstructure Evolution in La-β-Al_2O_3/Al_2O_3 Composites

Carmen Barrera-Solano* and Luis Esquivias*

Departamento de Física de la Materia Condensada, Universidad de Cádiz, Puerto Real, Cádiz 11510 Spain

Gary L. Messing*

Particulate Materials Center, Pennsylvania State University, University Park, Pennsylvania 16802

***In situ* development of La-β-Al_2O_3 (LBA) platelets in α-Al_2O_3 was studied as a function of the preparation method: a conventional solid-state reaction of commercial Al_2O_3 powder and $La(NO_3)_3$ as well as a sol–gel method starting with boehmite and the same La_2O_3 precursor. In both cases, homogeneous distribution of the reinforcing phase was achieved, and a noteworthy inhibition of Al_2O_3 grain growth resulted. However, samples prepared by solid-state reaction densified more easily than those prepared via sol–gel, but the formation of the LBA phase occurred at a lower temperature in samples prepared by the sol–gel approach. Results on the correlation of the onset of LBA grain growth and densification to microstructure are discussed.**

I. Introduction

STRUCTURAL ceramics are increasingly used in advanced technology and have displaced metallic alloys in some applications because of their excellent combination of properties, including high hardness, temperature stability, wear and chemical resistance, and strength. In many applications, brittle failure under mechanical or thermal stress is a major limitation of Al_2O_3 ceramics. Recently, there has been considerable research on composites in which crack growth can be stabilized or in which noncatastrophic failure occurs. For example, second phases with a high aspect ratio, such as fibers, whiskers, and platelets, can result in microstructural toughening. However, the high cost of the reinforcement materials poses a significant barrier to commercialization. Furthermore, processing problems, such as mixing heterogeneity and poor sintering, have added new challenges to the consistent manufacture of such materials.

A feasible, less-expensive, and safer alternative for microstructural reinforcement of Al_2O_3-based composites is the *in situ* formation and growth of highly anisotropic second-phase grains.[1–4] This technique favors homogeneous distribution, pressureless sintering, and thermal stability.

La_2O_3, when added to Al_2O_3, forms $LaAl_{11}O_{18}$ (LBA) by a solid-state reaction. LBA is a layered hexagonal aluminate. Roth and Hasko[5] assigned it the β-Al_2O_3 structure, but Lyi *et al.*[6] reported that it is a defective magnetoplumbite structure. Hamano *et al.*[7] determined that, in Al_2O_3/rare-earth systems, when sintering is done at a temperature higher than the eutectic point, the microstructure of the ceramics depends on the type of additives. The *in situ* formation of anisometric β-Al_2O_3 grains was first applied to abrasive grains.[8] It was found that the incorporation of small concentrations of La_2O_3 into Al_2O_3 by coprecipitation improved microstructural uniformity and the formation of $LaAl_{11}O_{18}$ after 2 h at 1200°C. Kang *et al.*[9] fabricated self-reinforced α-Al_2O_3 with different concentrations of $LaAl_{11}O_{18}$ to obtain better thermal stability than with Na-β-Al_2O_3 and to obtain a smaller grain size than with β‴-Al_2O_3 (~30 and ~5 μm for Na-β-Al_2O_3 and β‴-Al_2O_3, respectively). They showed that fracture toughness increased from 2.5 to 3.5 MPa·$m^{1/2}$ with increasing $LaAl_{11}O_{18}$ content. High strength (630 MPa) and high fracture toughness (6 MPa·$m^{1/2}$) were reported by Yasuoka *et al.*[10] for 20 vol% LBA/Al_2O_3 composites.

Ropp and Carroll[11] reported the kinetics of the solid-state reaction to form LBA between Al_2O_3 and La_2O_3. They found a perovskite-type aluminate ($LaAlO_3$) formed initially at 800°C that reacted with Al_2O_3 at higher temperature to form LBA:

$$La_2O_3 + Al_2O_3 \rightarrow 2LaAlO_3 \quad (1)$$

$$LaAlO_3 + 5Al_2O_3 \rightarrow LaAl_{11}O_{18} \quad (2)$$

Jantzen and Morgan reported that it was difficult to obtain phase-pure LBA even after heating $La(NO_3)_3 \cdot 6H_2O$ adsorbed on $Al(OH)_3$ at 1650°C for 115 h.[12]

The properties of LBA/Al_2O_3 composites depend on the second-phase concentration and preparation method. In this paper, we demonstrate how the preparation method affects the *in situ* formation of $LaAl_{11}O_{18}$. The processes are discussed in terms of phase development, $LaAl_{11}O_{18}$ crystallization, and microstructure development as a function of temperature for 30 vol% $LaAl_{11}O_{18}$/Al_2O_3 composites.

II. Experimental Procedure

Two basic methods for the synthesis and *in situ* growth of LBA in Al_2O_3 are investigated. Although all of the processes involve solid-state reaction, the first method is referred to as a solid-state reaction (SSR), because it is based on the conventional mixing of α-Al_2O_3 and a La_2O_3 precursor. To increase reaction kinetics and microstructure control, a sol–gel approach (SG) is also investigated.

(1) Solid-State Reaction

High-purity (>99.99%) α-Al_2O_3 powder (Baikalox™ SM8, Baikowski International Corp., Charlotte, NC) 0.3 μm in diameter was ultrasonically dispersed in distilled, pH 3 water and then mechanically stirred. The appropriate amount of $La(NO_3)_3 \cdot 6H_2O$ (Johnson Matthey Electronics, Wayne, PA) was added to the Al_2O_3 slurry to yield a net composition of 30 vol% LBA and 70 vol% α-Al_2O_3. The mixture was mechanically stirred for 24 h, and a portion was dried on a hot plate at 100°C while stirring. The resultant powder was designated as SSR1. Aqueous NH_3 was added to the remaining suspension at

P. F. Becher—contributing editor

Manuscript No. 191273. Received January 16, 1997; approved September 18, 1998.

*Member American Ceramic Society.

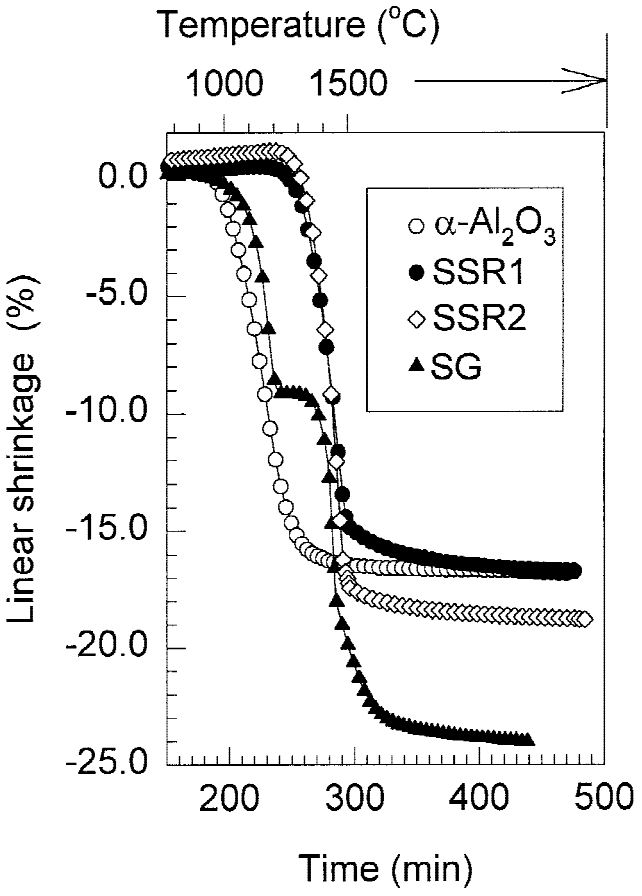

Fig. 1. Shrinkage behavior versus temperature for 300°C/h and a 3 h dwell at 1500°C.

pH 10 in order to make the dry slurry easier to mill and to precipitate $La(OH)_3$. This batch was designated as SSR2. The dried powders were calcined in air at 750°C for 2 h and hand-ground in an alumina mortar before and after calcination. The calcined powders were uniaxially pressed at 160 MPa.

(2) Sol–Gel Method

A boehmite sol (Disperal Sol P2, Condea, Hamburg, Germany) was dispersed at pH 4.5 and seeded with 1.75 wt% of 0.1 μm diameter Al_2O_3.[13] The seeded sol was mixed with the appropriate amount of $La(NO_3)_3 \cdot 6H_2O$ to yield an Al_2O_3/LBA volume ratio of 7/3 and stirred for 24 h at room temperature. The sol was heated at 80°C until gelled. The gel was milled in an alumina mortar, and the resulting powder was sieved to <354 μm (−45 mesh). Pellets were uniaxially pressed at 70 MPa and cold isostatically pressed at 275 MPa before calcination at 750°C for 2 h. These samples were designated as SG.

Densities of the samples were determined by geometry. When the relative density was >0.92, density was measured by the Archimedes method. Phase development was characterized by DTA and XRD. Pellet shrinkage during sintering was monitored by thermal mechanical analysis (TMA). Both DTA and TMA were performed at 300°C/h. Samples were heated at 800°C for 2 h before TMA. Samples were sintered at 60°C/h up to 1500°C and then held for 3 h dwell at 1500°C. Fourier transform infrared (FTIR) spectra were obtained using pellets of KBr mixed with 3 wt% heat-treated powders. Microstructures of polished and thermally etched samples were examined by SEM and energy dispersive spectroscopy (EDS).

III. Results and Discussion

In the case of the SSR1 sample, there is an endothermic reaction at 290°C, which we attribute to nitrate decomposition, because programmed thermal decomposition analysis (heating rate 10°C/min) coupled with mass spectroscopy shows that NO evolves at 400°C as a consequence of $La(NO_3)_3 \cdot 6H_2O$ decomposition.[14] No $La(NO_3)_3$ decomposition peaks are seen for the SSR2 sample, because $La(OH)_3$ precipitates when slurry pH is increased from 3 to 10. DTA of the sol–gel samples shows broad endothermic peaks at 405°–410°C due to the boehmite → γ-Al_2O_3 transformation.[15] $La(NO_3)_3$ gradually decomposes by a single-stage reaction at ~400°C instead of the characteristic two-stage process of pure $La(NO_3)_3 \cdot 6H_2O$.[14]

No notable features are observed in the shrinkage plots of the samples up to 950°C (Fig. 1). At this temperature, the pure α-Al_2O_3 shrinkage rate increases but then decreases above 1300°C. The SSR1 and SSR2 samples do not start to shrink until >1275°C because of the presence of a second phase.

There is no shrinkage in the SG specimens below 750°C as a result of the AlOOH → γ-Al_2O_3 transformation, because the samples are calcined at 750°C prior to TMA. Shrinkage in the SG samples starts at ~1000°C as a result of the transformation of the transition Al_2O_3 to α-Al_2O_3 but stops at ~1175°C. Linear shrinkage in the SG samples is 8.4%, which is in proportion to the boehmite concentration in the initial system. The α-Al_2O_3 seeds act as nucleation sites for the α-Al_2O_3 transformation in boehmite gels.[16] However, the transformation temperature is only slightly affected by the seed particles in the presence of La^{3+} and the LBA precursor particles. This observation agrees with reports on the increased thermal stabilization of transition Al_2O_3 in La_2O_3-doped transition Al_2O_3.[17,18] In addition, the sintered density of the SG samples does not appear to be affected by the presence of α-Al_2O_3 seed particles. The SG samples densify over a narrower temperature range relative to both pure α-Al_2O_3 and SSR samples, because La^{3+} inhibits the transformation of transition Al_2O_3 to α-Al_2O_3 and its sintering.

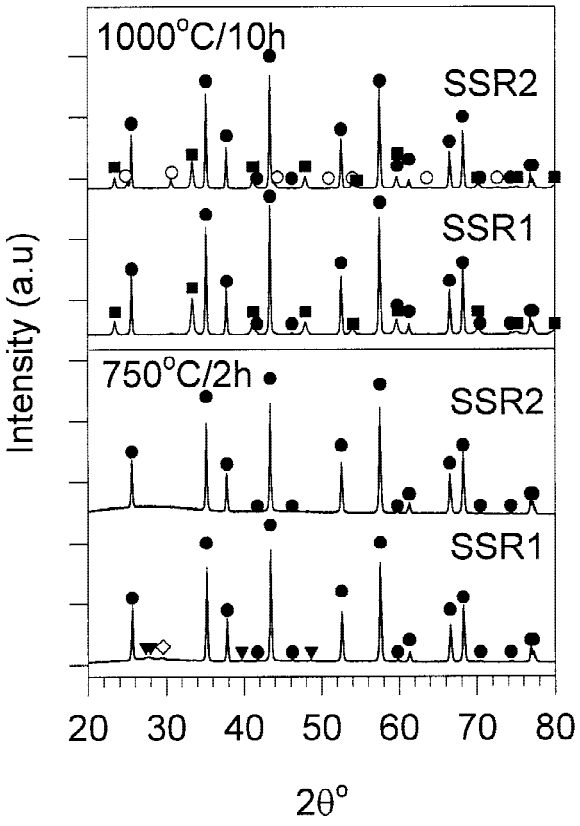

Fig. 2. Comparison of XRD patterns of SSR samples calcined at 750°C and sintered at 1000°C ((●) α-Al_2O_3, (■) $LaAlO_3$, (❍) $LaCO_3OH$, (▼) peaks of $La(OH)_3$ that can be seen in the SSR1 sample pattern and (◇) tiny peak observed at 2θ = 29.5° that seemingly corresponds to $La_2O_2CO_3$).

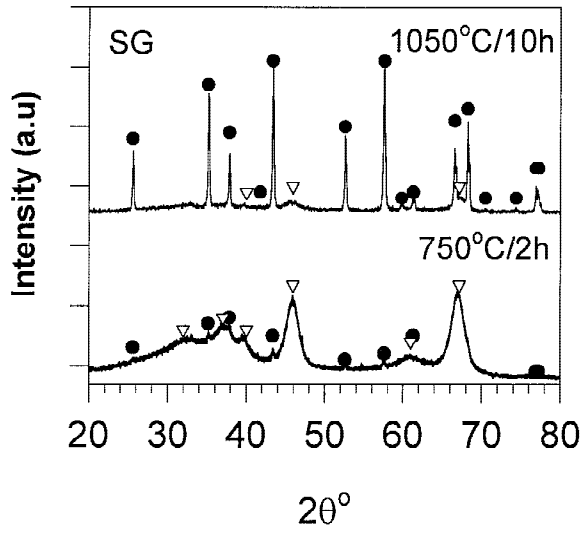

Fig. 3. Comparison of XRD patterns of SG samples calcined at 750°C and sintered at 1000°C ((●) α-Al_2O_3, (■) $LaAlO_3$, and (▽) γ-Al_2O_3).

The XRD spectra of SSR calcined samples do not show significant differences (Fig. 2). Very small peaks of carbonates and hydroxides are observed that are difficult to explain because no care was taken to preserve the samples from the atmosphere during the manipulation. As is well-known, evolution of La_2O_3 exposed to the atmosphere is very fast, leading to the formation of hydroxide and hydroxycarbonates.[19,20] In both patterns, the α-Al_2O_3 peaks appear above the background because of the presence of an amorphous phase (wider in the case of SSR2 sample), likely formed by the reprecipitated dissolved Al_2O_3 and lanthanum hydroxycarbonates. There are no major differences between the FTIR spectra of calcined powders of SSR1 and SSR2 preserved from the atmospheric moisture. Only the bands corresponding to hydroxyls are slightly stronger in the SSR2 sample spectrum because of the higher concentration of these groups in the SSR2 sample. This indicates that lanthanum is not as homogeneously distributed in SSR2 as in SSR1, where only α-Al_2O_3 and $LaAlO_3$ peaks appear after 1100°C calcination.

Only γ-Al_2O_3 and traces of α-Al_2O_3 are present in the SG sample calcined at 750°C (Fig. 3). In the SSR samples, $LaAlO_3$ crystallizes at <1000°C (Fig. 2) but is not present after heating at 1450°C (Fig. 4). Likewise, in SG samples, $LaAlO_3$ is formed between 1050° and 1100°C (Fig. 5). LBA peaks can be noted in the spectrum at 1100°C (Fig. 5). The temperature interval for the existence of perovskite in SG is extremely short, and Rietveld analysis shows only 2.2 vol% exists at 1100°C and 0.7 vol% at 1350°C.[21] This agrees with Cinibulk's[22] finding that the sol–gel route could be used to produce LBA in much shorter processing times. However, whereas Cinibulk finds a yield of ~85% on calcining for 2 h at 1450°C, our XRD analysis indicates a yield of 100% on calcining for 5 h at 1300°C. No isolated grains of $LaAlO_3$ are detected, and no peaks are observable in the DTA spectra for the formation of either $LaAlO_3$ or LBA. There is no sign of La_2O_3 crystallization in the XRD

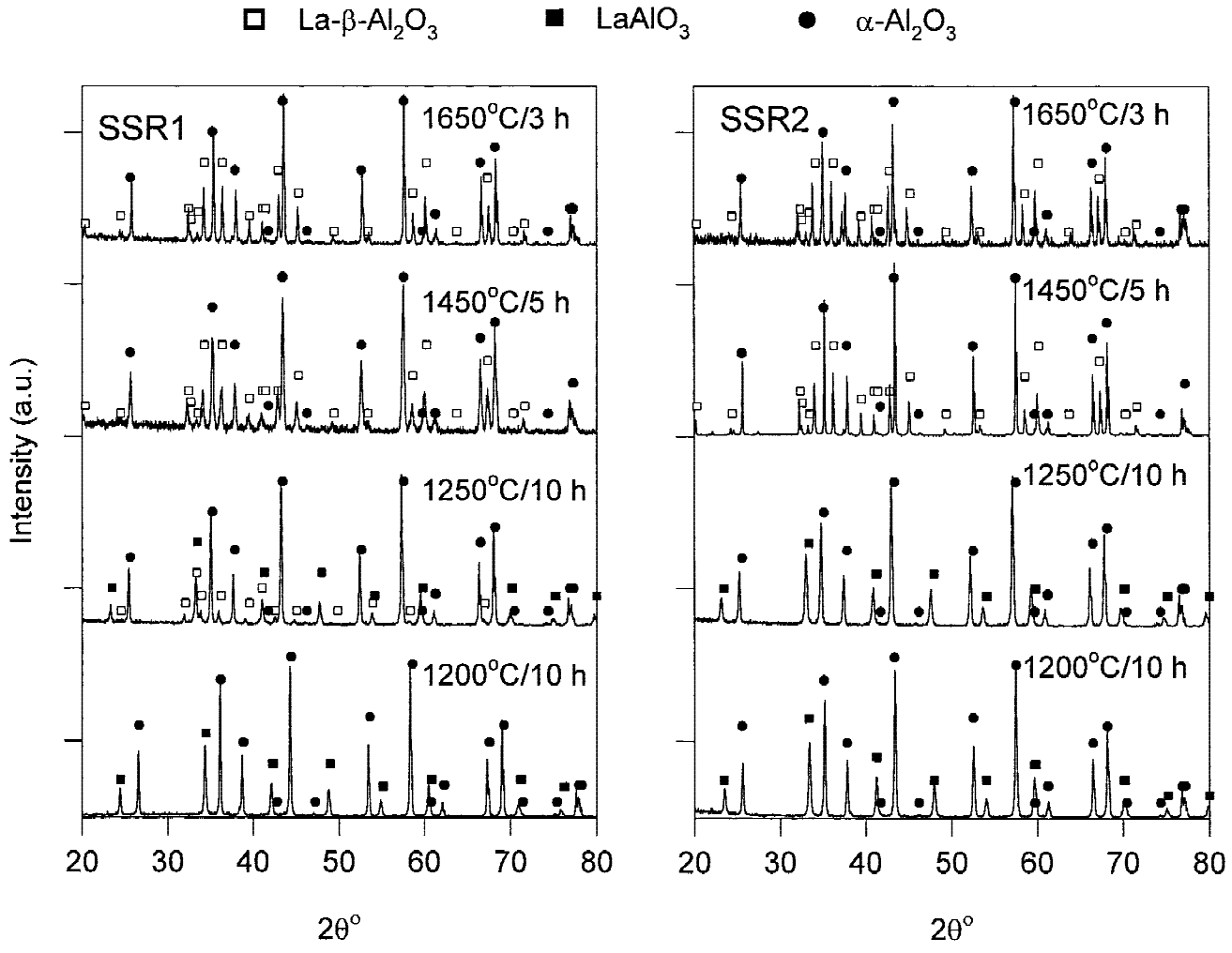

Fig. 4. Comparison of XRD patterns of SSR samples as a function of temperature.

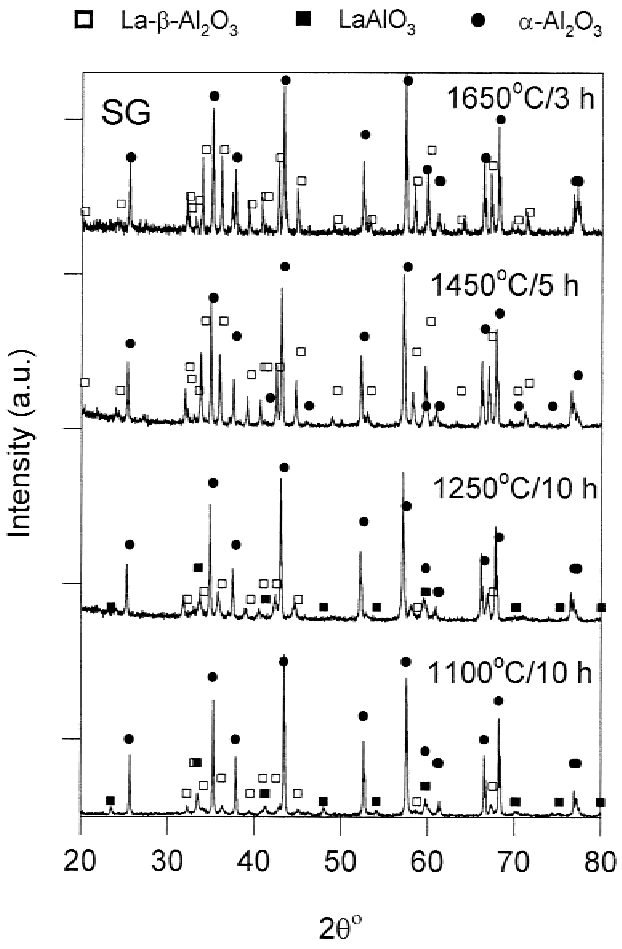

Fig. 5. Comparison of XRD patterns of SG samples as a function of temperature.

patterns. Interestingly, nearly identical XRD patterns are obtained for all samples, independent of preparation method after heating at 1450°C for 5 h (Figs. 4 and 5).

Figure 6 compares the bulk densities of the LBA/Al_2O_3 composites as a function of the preparation process. The pure Al_2O_3 sample is included to evaluate the effect of La_2O_3 on sintering. The theoretical density of the 30 vol% LBA composite is 4.04 g/cm^3, as calculated from the theoretical densities of Al_2O_3 (3.986 g/cm^3) and LBA (4.17 g/cm^3).[6] The 100% Al_2O_3 sample reaches 93% density at 1300°C, whereas the sol–gel-derived LBA-containing sample is ~61% dense, and the SSR1 and SSR2 samples are 71% and 74% dense, respectively. Subsequent densification depends dramatically on the preparation method. The formation of platelets at a lower temperature restrains densification because platelet geometry does not favor efficient particle packing (Fig. 7). As evidenced by the plateau (Figs. 1 and 6) between 70% and 75% density in the density curves of SG samples, LBA crystal growth, which initiates at ~1350°C,[19] significantly hinders densification. This plateau has its counterpart in SSR samples. These density values are relative to those of a composite with nominal relative concentrations. This criterion leads to a relative density overestimation for samples containing $LaAlO_3$ (6.52 g/cm^3) that are sintered at temperatures <1300°C. A content of 10 vol% of $LaAlO_3$ in SSR samples represents an ~6% overestimation of their actual relative density. In the SG sample, no perovskite is observed at >1100°C. After phase formation is complete, further densification of SSR samples to 94% appears to be unhindered by the presence of the new phase. However, SG does not reach >95% density until 1650°C, seemingly because the green body particle aggregates are much larger than in SSR.

LBA grains have been reported to be either platelet-[9] or

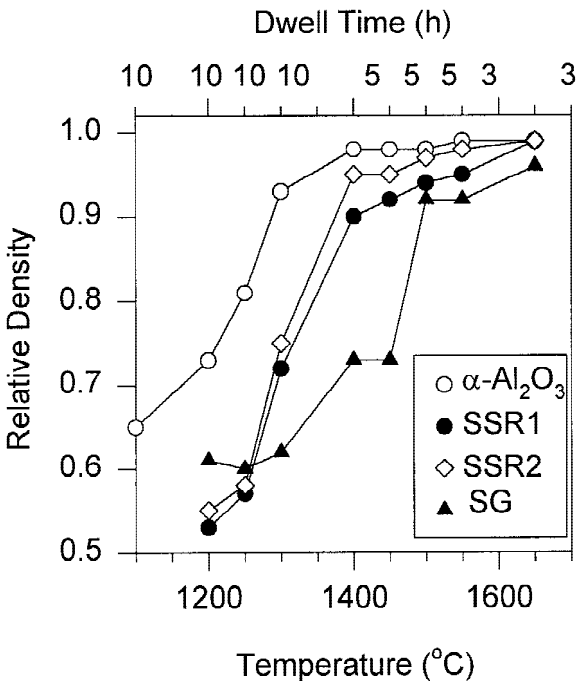

Fig. 6. Densities of SG and SSR samples after various hold times at temperatures.

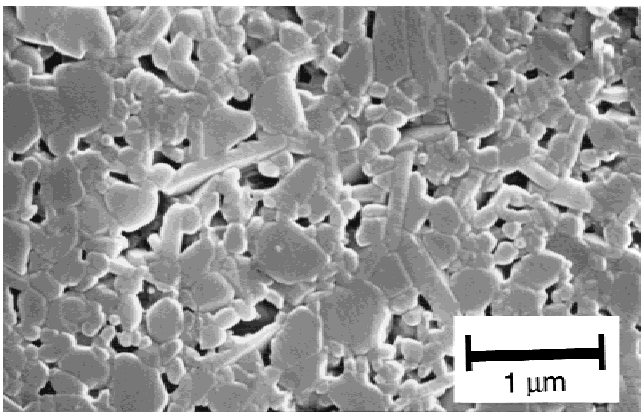

Fig. 7. Microstructure of SG sintered at 1350°C for 5 h.

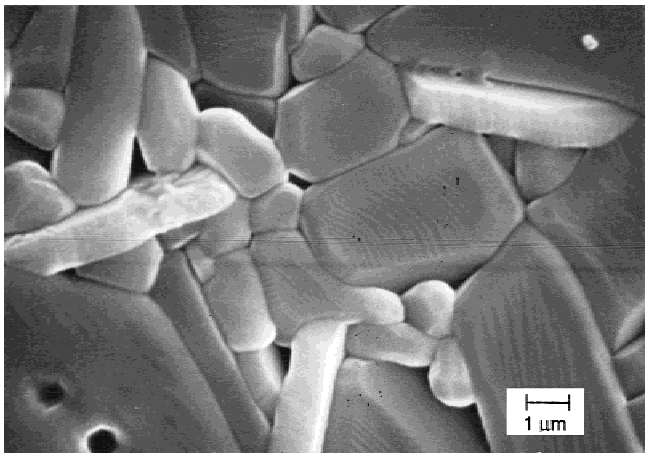

Fig. 8. SEM showing evidence of plateletlike structure of the anisometric phase. Micrograph corresponds to SSR1 sintered at 1650°C for 3 h.

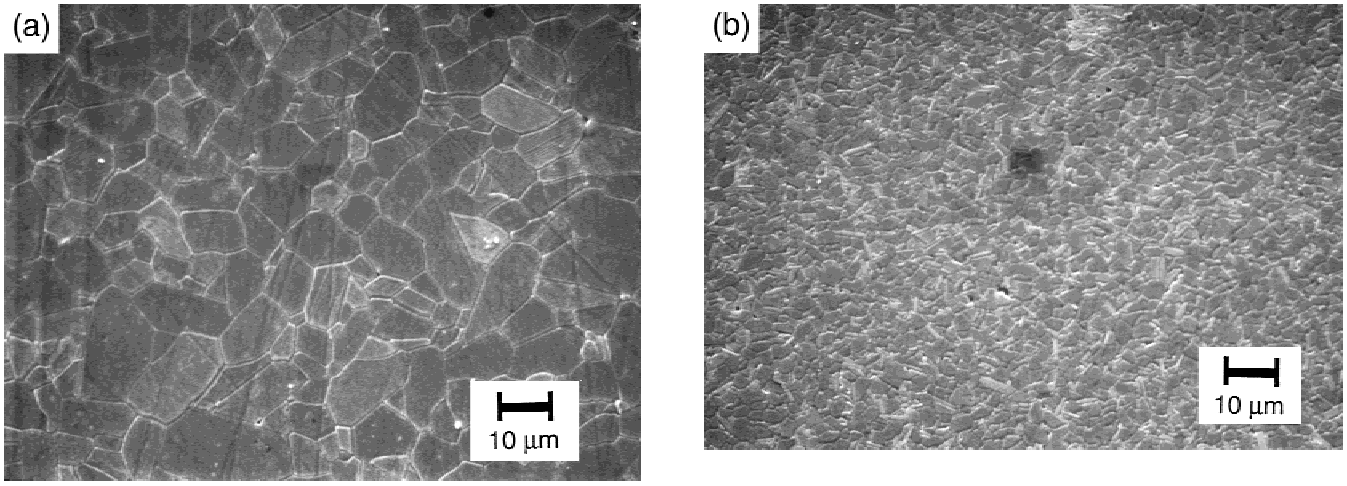

Fig. 9. Micrographs on polished and thermally etched surfaces of sintered bodies at 1650°C for 3 h, showing grain growth inhibition for the α-Al_2O_3 matrix as a consequence of LBA formation: (a) pure α-Al_2O_3 and (b) SSR1.

needle-shaped.[23] Recently, An *et al.* have reinforced *in situ* Al_2O_3 with calcium hexaluminate, finding that the morphology of this hexaluminate depends on the precursor calcium-containing powder.[24] The micrograph in Fig. 8 clearly demonstrates the platelet shape of the LBA grains when $La(NO_3)_3 \cdot 6H_2O$ is used as lanthanum precursor for both SSR and SG methods. LBA grains are easily distinguished, because they contain lanthanum, which is very absorbent, resulting in bright images. The sintered bodies comprise equiaxed grains of different sizes, which are classified as type 1 (diameter > 0.5 μm),

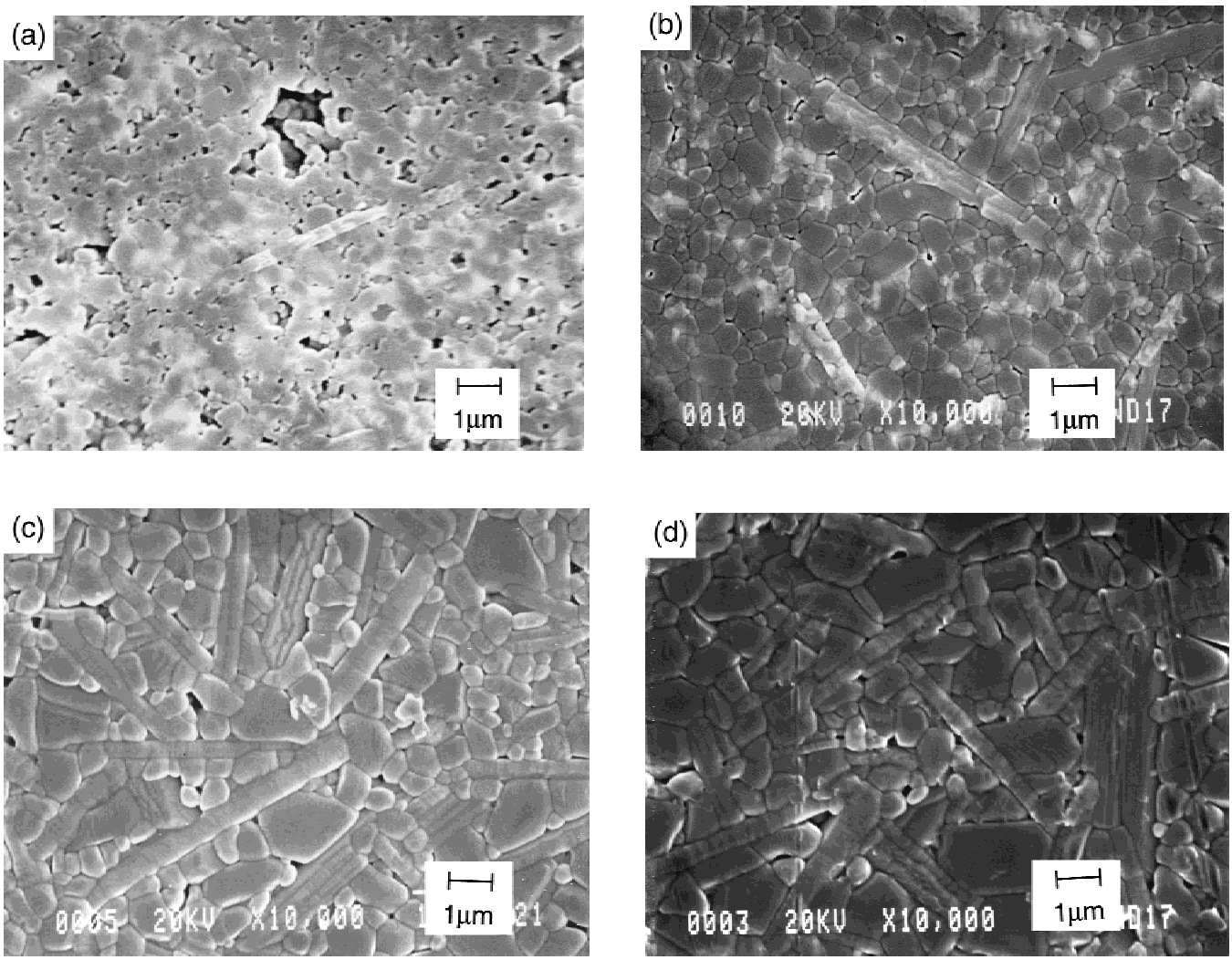

Fig. 10. Micrographs showing the microstructure of LBA platelet formation in the SSR1 sample: (a) sintered at 1350°C for 10 h, (b) sintered at 1400°C for 5 h, (c) sintered at 1450°C for 5 h, and (d) sintered at 1500°C for 3 h.

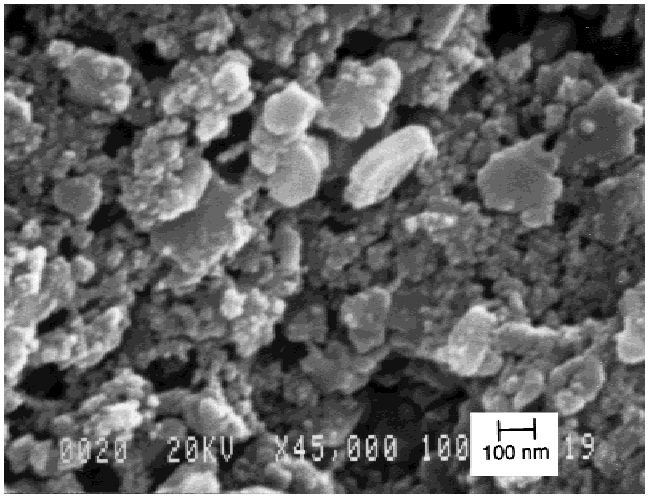

Fig. 11. Platelets in SG heat-treated at 1050°C for 10 h.

type 2 (diameter < 0.5 μm), and type 3 (elongated grains). EDS spectra of grains of different aspect ratio show that their morphology is related to chemical composition. The type 1 grains are determined to be Al_2O_3, whereas both the smaller equiaxed grains (type 2) and platelet grains contain lanthanum. Based on EDS peak heights and XRD data, the anisometric grains (type 3) are LBA, and equiaxed small grains are $LaAlO_3$. EDS spectra of those readily detected as hexagonal exhibit the same relative lanthanum peak height as type 3 LBA grains.

The first consequence of adding lanthanum on microstructure evolution is the inhibition of grain growth (Fig. 9). The micrographs demonstrate that α-Al_2O_3 compacts sintered at 1650°C for 3 h have an average grain size of 8.2 μm, in contrast to the LBA-containing sample (SSR1) where α-Al_2O_3 grain size is ~1.8 μm and uniformly distributed LBA platelets occur.

The micrographs of SSR1 samples clearly illustrate the dependence of grain size and platelet formation on sintering temperature (Fig. 10). 1350°C is the lowest temperature at which platelets are detected in the SSR1 sample, whereas, in the case of SG, they are observed at a temperature ≥1050°C (Fig. 11). In SSR1, grain growth proceeds in two stages: sharp growth between 1400° and 1450°C followed by slow growth to 1650°C. The same intense growth is observed for the SG specimens. In this case, platelets are <1 μm in width up to 1350°C (Fig. 7). Grain growth in the SSR2 is similar to the above description up to 1550°C, but there is a remarkable increase from this temperature to 1650°C.

The micrographs in Fig. 9(b) and Fig. 12 show that hydroxide precipitation of lanthanum affects microstructure development in the SSR samples. Both LBA and α-Al_2O_3 grains are smaller and more homogeneously distributed in SSR1 than in SSR2. The difference is believed to be due to the difference in LBA phase formation. In SSR1, LBA begins to form at 1250°C; however, in SSR2, more $LaAlO_3$ exists at 1250°C, but there is no LBA (Fig. 4). The difference in phase formation in these two systems could be a result of more homogeneous mixing and better retention of homogeneity in the dried SSR1. The formation of perovskite-type lanthanum aluminate (La/Al ratio 1/1) is more favorable in areas with a high concentration of lanthanum (Eq. (1)). However, the formation of LBA requires an Al_2O_3/perovskite molar ratio of 5/1 (Eq. (2)). Thus, at low temperature, the capacity of LBA formation is moderate in lanthanum-rich (Al_2O_3-poor) areas. NH_3 fluxing of the SSR2 (pH 10) results in a nonuniform distribution of lanthanum, creating areas under stoichiometry to form hexaluminate. Only at temperatures near 1400°C is diffusion sufficiently high for complete reaction to form LBA. In this sample, the concentration of $La(OH)_3$ in some areas relieves inhibition of Al_2O_3 grain growth, where the lanthanum concentration is low. In such a site, the Al_2O_3 grains grow, and the density is >0.94 of theoretical at 1400°C, which is 100°C below the temperature required for SSR1. In contrast, in SSR1, dissolved La^{3+} and Al^{3+} precipitate on the surface of the remaining α-Al_2O_3 particles in solution, favoring a homogeneous distribution of the reactant and the formation of $LaAl_{11}O_{18}$ at 1250°C. Similarly, SG has a homogeneous microstructure, although it is not as fine as in the SSR1 sample (Fig. 12).

IV. Conclusions

(1) The temperature at which the La-β-Al_2O_3 is formed depends on the method of preparation. We have shown evidence that the shape of this anisotropic phase is plateletlike. In the sol–gel sample, La-β-Al_2O_3 can be observed at 1050°C, 300°C lower than when prepared by solid-state reaction.

(2) The growth of platelets controls the densification process. When sharp platelet growth is observed in the interval 1400°–1450°C, no noticeable density increase is observed. The formation of platelets at low temperature, using the sol–gel method, restrains densification, because platelet geometry does not favor packing. This platelet formation combined with inhibited Al_2O_3 grain growth results in poor density of samples sintered at <1450°C.

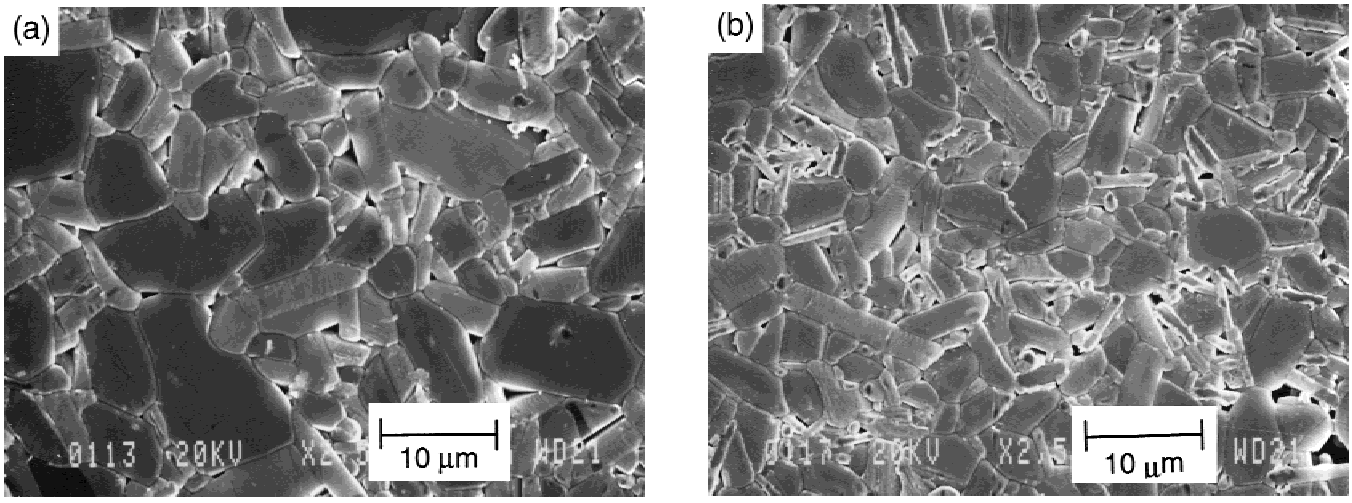

Fig. 12. Micrographs of samples sintered at 1650°C for 3 h: (a) SSR2 and (b) SG.

(3) The finest microstructure is achieved in the SSR1 sample.

(4) Nearly identical XRD patterns are obtained for all samples, independent of preparation method after heating at 1450°C for 5 h. However, samples prepared by solid-state reaction densify more easily, but those prepared via sol–gel experience shrinkage in a narrower temperature interval.

(5) Homogeneous distribution of platelets results from both methods, especially in solid-state reaction without forcing the precipitation of $La(OH)_3$. The sample seeded with LBA precursor results in a very inhomogeneous sample with two types of microstructures.

References

[1]R. A. Cutler, R. J. Mayhew, K. M. Prettyman, and A. V. Virkar, "High-Toughness Ce-TZP/Al_2O_3 Ceramics with Improved Hardness and Strength," *J. Am. Ceram. Soc.*, **74** [1] 179–86 (1991).

[2]P. F. Becher, "Microstructural Design of Toughened Ceramics," *J. Am. Ceram. Soc.*, **74** [2] 255–69 (1991).

[3]J. F. Tsai, U. Chong, N. Ramachandran, and D. K. Shetty, "Transformation Plasticity and Toughening in CeO_2-Partially-Stabilized Zirconia–Alumina Composites Doped with MnO," *J. Am. Ceram. Soc.*, **75** [5] 1229–38 (1992).

[4]P.-L. Chen and I-W. Chen, "In-Situ Alumina/Aluminate Composites," *J. Am. Ceram. Soc.*, **75** [9] 2610–12 (1992).

[5]R. S. Roth and S. Hasko, "Beta-Alumina Type Structure in the System Lanthana–Alumina," *J. Am. Ceram. Soc.*, **41** [4] 146 (1958).

[6]N. Lyi, Z. Inoue, S. Takekawa, and S. Kimura, "The Crystal Structure of Lanthanum Aluminate," *J. Solid State Chem.*, **54**, 70 (1984).

[7]K. Hamano, S. Ohta, and Y. Ozaki, "The Effect of Rare Earth Oxides on Sintering of Alumina" (in Jpn.), *Yogyo Kyokaishi*, **87** [12] 63241 (1979).

[8]L. D. Monroe and W. P. Wood, "Abrasive Grits Formed of Ceramic Containing Oxides of Aluminum and Rare-Earth Metal, Method of Making and Products Made Therewith," U.S. Pat. No. 4 881 951, Nov. 21, 1989.

[9]S. W. Kang, J.-W. Ko, and H.-D. Kim, "Formation of La-β-Aluminate in α-Alumina Matrix and its Influence on Mechanical Properties," *J. Korean Ceram. Soc.*, **29** [1] 23–28 (1992).

[10]M. Yasuoka, K. Hirao, M. Brito, and S. Kanzaki, "High-Strength and High-Fracture-Toughness Ceramics in the $Al_2O_3/LaAl_{11}O_{18}$ Systems," *J. Am. Ceram. Soc.*, **78** [7] 1853–56 (1995).

[11]R. C. Ropp and B. Carroll, "Solid State Kinetics of $LaAl_{11}O_{18}$," *J. Am. Ceram. Soc.*, **63**, 416–19 (1980).

[12]Powder Diffraction File, Card No. 34-467, International Centre for Diffraction Data, Newtown Square, PA, 1983.

[13]M. Kumagai and G. L. Messing, "Controlled Transformation and Sintering of a Boehmite Sol–Gel by α-Al_2O_3," *J. Am. Ceram. Soc.*, **68** [9] 500–505 (1985).

[14]H. Vidal, "Caracterización de Óxidos Lantánidos Dispersos Sobre Sílice" (Characterization of Lanthanide Oxides Dispersed in Silica); Microthesis. Universidad de Cádiz, Cadiz, Spain, 1992.

[15]J. L. McArdle and G. L. Messing, "Seeding with γ-Alumina for Transformation and Microstructure Control in Boehmite-Derived α-Alumina," *J. Am. Ceram. Soc.*, **69** [5] C-98–C-101 (1986).

[16]M. Kumagai and G. L. Messing, "Enhanced Densification of Boehmite Sol–Gels by α-Alumina Seeding," *J. Am. Ceram. Soc.*, **67** [11] C-230–C-231 (1984).

[17]H. Schapper, E. B. M. Doesburg, and L. L. Van Reijen, "The Influence of Lanthanum Oxide on the Thermal Stability of Gamma Alumina Catalyst Support," *Appl. Catal.*, **7**, 211–20, (1983).

[18]S. Matsuda, A. Kato, M. Mizumoto, and H. Yamashita, "A New Support for Catalytic Combustion"; p. 879 in *8th International Congress on Catalysis*, Proceedings, Vol. 4, (Berlin, Germany, July 1984).

[19]S. Bernal, F. J. Botana, R. García, and J. M. Rodríguez-Izquierdo, "The Behaviour of Rare Earth Sequioxides Exposed to Atmosphere Carbon Dioxide and Water," *React. Solids*, **4**, 23–40 (1987).

[20]S. Bernal, F. J. Botana, F. Ramírez, and J. M. Rodríguez-Izquierdo, "Solid State Chemistry of the Preparation of Lanthanum-Supported Metal Catalyst. Study of the Impregnation Step," *J. Mater. Sci.*, **22**, 3793–800 (1987).

[21]C. Barrera-Solano, L. Esquivias, and F. L. Cumbrera, "Rietveld Analysis of La-β-Alumina/Alumina Composites Prepared from Boehmite Gels"; in *Sol–Gel '97*, 9th International Workshop on Glasses, Ceramics, Hybrids and Nanocomposites from Gels, (Sheffield, U.K., Aug. 31–Sept. 5, 1997).

[22]M. K. Cinibulk, "Synthesis and Characterization of Sol–Gel-Derived Lanthanum," *J. Mater. Res.*, **10** [1] 71–76 (1995).

[23]T. Fujii, H. Muragaki, and H. Hirano, "Microstructure Development and Mechanical Properties of Ce-TZP/La-β-Alumina Composites"; pp. 693–98 in Ceramic Transactions, Vol. 22, *Ceramic Powder Science IV*. Edited by S. Hirano, G. L. Messing, and H. Hausner. American Ceramic Society, Westerville, OH, 1991.

[24]L. An, H. M. Chan, and K. K. Chan, "Control of Calcium Hexaluminate Grain Morphology in *In situ* Toughened Ceramic Composites," *J. Mater. Sci.*, **31**, 3223–29 (1996). □